Journal of Power Sources 196 (2011) 1955–1966

Contents lists available at ScienceDirect

Journal of Power Sources

journal homepage: www.elsevier.com/locate/jpowsour

Chemical degradation of five elastomeric seal materials in a simulated and an accelerated PEM fuel cell environment

Chih-Wei Lin[a,b], Chi-Hui Chien[a], Jinzhu Tan[c], Yuh J. Chao[b,*], J.W. Van Zee[d]

[a] Department of Mechanical and Electro-Mechanical Engineering, National Sun Yat-Sen University, Kaohsiung 804, Taiwan, ROC
[b] Department of Mechanical Engineering, University of South Carolina, Columbia, SC 29208, USA
[c] College of Mechanical and Power Engineering, Nanjing University of Technology, Nanjing, Jiangsu 210009, China
[d] Department of Chemical Engineering, University of South Carolina, Columbia, SC 29208, USA

ARTICLE INFO

Article history:
Received 18 August 2010
Received in revised form 1 October 2010
Accepted 4 October 2010
Available online 3 November 2010

Keywords:
ATR-FTIR
Degradation
Leachants
Elastomeric gaskets
PEM fuel cell
Weight loss

ABSTRACT

Polymer electrolyte membrane (PEM) fuel cell stack requires gaskets and seals in each cell to keep the hydrogen and air/oxygen within their respective regions. The stability of the gaskets/seals is critical to the operating life as well as the electrochemical performance of the fuel cell.

Chemical degradation of five elastomeric gasket materials in a simulated and an aggressive accelerated fuel cell solution at PEM operating temperature for up to 63 weeks was investigated in this work. The five materials are copolymeric resin (CR), liquid silicone rubber (LSR), fluorosilicone rubber (FSR), ethylene propylene diene monomer rubber (EPDM), and fluoroelastomer copolymer (FKM).

Using optical microscopy, topographical changes on the sample surface due to the acidic environment were revealed. Weight loss of the test samples was monitored. Atomic absorption spectrometer analysis was performed to study the silicon, calcium, and magnesium leachants from the materials into the soaking solution. Attenuated total reflection-Fourier transform infrared (ATR-FTIR) spectroscopy was employed to study the surface chemistry of the materials before and after exposure to the simulated fuel cell environment over time.

Among the five materials studied, CR and LSR in the accelerated solution are not as stable as the other three materials. FSR appears to be the most stable.

1. Introduction

A single proton exchange membrane (PEM) fuel cell consists of end plates, current collectors, flow channel plates, gaskets, gas diffusion layers, and a membrane electrode assembly (MEA). All these components must be carefully assembled and sealed with gaskets or seals around the perimeters.

A typical PEM fuel cell stack used in automotive application may include over 100 cells and therefore large linear perimeter of exposure for the seals or gaskets. If any seal degrades or fails during operation or standby, the reactant gases (O_2 and H_2) can leak overboard or mix each other directly. This will affect the overall operation and performance of the fuel cells.

Selection of a gasket for PEM fuel cells involves many factors [1]. Both the cost, including raw material, fabrication, installation, labor, equipment, overhead, and depreciation of equipment, and the engineering functionality of the seal material have to be considered. Typically, elastomeric materials are used as seals or gaskets as they are relatively less expensive and easy in fabrication. These elastomeric materials when used as seals in PEM fuel cells are exposed to acidic liquid solution, humid air, coolant and hydrogen, as well as mechanical stress. The long-term stability and durability of these materials are therefore critical to both sealing and the electrochemical performance of the fuel cells.

In the open literature, there are many reports in which the major emphasis is on thermal or irradiative degradation of polymeric materials [2–18]. For instance, Youn and Huh [4] reported the surface degradation of silicone rubber and EPDM under accelerated ultraviolet weathering conditions. A severe degradation of silicone elastomer in a sub-station environment was studied by Liu et al. [18]. A review on the effects and degradation process of silicones in outdoor environments can be found in Graiver et al. [19]. Mitra et al. [20,21] investigated the chemical degradation of cross-linked EPDM rubber in a 20% Cr/H_2SO_4 acidic environment. Time-dependent chemical degradation of a fluoroelastomer in an alkaline environment was reported in Refs. [22,23]. Achenbach [24–26] studied seal life using numerical simulation for stress relaxation and degradation in different environments. Kim et al. [27] presented degradation results of nitrile rubber (NBR) compound-based rubber gaskets in acidic environments. More fun-

* Corresponding author. Tel.: +1 803 7775869; fax: +1 803 7770106.
E-mail address: chao@sc.edu (Y.J. Chao).

0378-7753/$ – see front matter © 2010 Elsevier B.V. All rights reserved.
doi:10.1016/j.jpowsour.2010.10.012

Table 1
Material properties.

Material	CR[a]	FSR[a]	LSR[a]	EPDM[b]	FKM[c]
Sample thickness (mm)	1.5	2.0	2.0	2.0	2.0
Color	White	Straw yellow	Slate gray	Black	Black
Hardness (Shore A)	60–75	35–45	66	40–90	75
Elongation (%)	400	≥300	451	100–600	200
Relative density ($g\,cm^{-3}$)	1.08	1.43	1.14	0.90 to >2.00	2
Tear strength (ppi)	241	100	241	200	144
Tensile strength (Mpa)	9	8	10	25	9
Work temperature (°C)	−40 to 316	−60 to 220	−40 to 205	−20 to 250	−7 to 200

[a] Dow Corning Company [51].
[b] AZo Journal of Materials Online [54].
[c] ThomasNet [56].

damental studies have been performed by Gillen et al. [28–40] on polymeric materials to reveal their degradation mechanisms and develop seal life models.

Although there is a substantial literature discussing chemical degradation of elastomeric gasket materials, only a few are concerned with the degradation and its mechanisms in PEM fuel cell environment. Schulze et al. [41] investigated the degradation of seals in PEM fuel cells during fuel cell operation. Tan et al. [42–49] studied the chemical and mechanical degradation of silicone rubber, fluoroelastomer, and EPDM materials exposed to a high concentration PEM fuel cell solution in accelerated tests. The effects of compression and gas diffusion layers on the performance of a PEM fuel cell were examined by Lee et al. [50].

In this study, chemical degradation of five elastomeric seal materials in a simulated and an accelerated fuel cell environments was investigated. Although the accelerated durability test (ADT) solution may not simulate all end-of-life fuel cell environments, we believe it to be an aggressive solution suitable for a worst-case scenario. The second solution (regular) is close to what is inside an operating PEM fuel cell. Specimens were aged at 80 °C which is near the operating temperature of typical PEM fuel cells. Surface conditions of the aged samples were examined using optical microscopy. Weight loss was monitored at selected exposure times. ATR-FTIR spectroscopy was used to detect chemistry changes on the surface. Atomic absorption spectrometry was used to identify the chemicals leached from the gasket samples into the soaking solution. The objective of the present study is to investigate and to compare the degrees of chemical degradation, if any, of the five potential gasket/seal materials in simulated PEM environment. The results are useful in evaluation and selection of gasket/seal materials for PEM fuel cells applications.

2. Experimental descriptions

2.1. Materials and simulated fuel cell environment

Five elastomeric sealing materials, namely, copolymeric resin (CR), fluorosilicone rubber (FSR), liquid silicone rubber (LSR), ethylene propylene diene monomer rubber (EPDM), and fluoroelastomer copolymer (FKM), were used in this study. According to our industrial contacts, these materials appeared to have the potential to be used in fuel cells prior to this study. Relevant properties of these materials are shown in Table 1. A brief introduction of these materials is provided below:

(1) Copolymeric resin (CR) is a silicone resin. It's formulation composed mostly of $(Me_2SiO)_x(Me_2SiO_3)_y$. The curing sites contain SiOSi units. The filler is calcium carbonate. The curing of this material is dried from solvent. The product number of the material number is Dow Corning CF-0020 [51]. Note that CR here is not neoprene rubber, as commonly implied in industry.

(2) Liquid silicone rubber (LSR) is a two-part silicone based, liquid injection molded material which is mixed and rapidly heat-cured to form elastomeric components. Part A is composed of polymers $ViMe_2SiO(Me_2SiO)_x(MeViSiO)_ySiMe_2Vi$, fillers (such as SiO_x and Ca_2CO_3), and platinum catalyst (there are some very minor promoters such as $HOMe_2SiO(Me_2SiO)_xSiMe_2OH$). Part B has essentially the same formulation except it has an extra component $Me_3Si(Me2SiO)_x(MeHSiO)_ySiMe_3$. The crosslinking sites in gaskets have $Si–CH_2CH_2–Si$ bond. The crosslinking reaction mechanism is hydrosilylation [52,53]. The product number for this material is Dow Corning Silastic® 4-2010 LSR [51]. This same material designated as Silicone S was studied by Tan et al. [42–44,47–48].

(3) Fluorosilicone rubber (FSR) has a very similar formulation to LSR except that the polymers, rather than having Me_2SiO units, have $(CF_3CH_2CH_2)MeSiO$ units. These polymers are 100% fluorosilicone elastomer. The crosslink site also contains $Si–CH_2CH_2–Si$ unit [51]. The product number for this material is Dow Corning FL-40-9201.

(4) Ethylene propylene diene monomer rubber (EPDM) is a synthetic rubber. It exhibits satisfactory compatibility with fireproof hydraulic fluids, ketones, hot and cold water, and alkalis; but is not compatible with most oils, gasoline, kerosene, aromatic and aliphatic hydrocarbons, halogenated solvents, and concentrated acids [54]. This EPDM material consists of ethylene and propylene co-monomers having 5-ethylidene-2-norbornene (ENB) as diene. It's composed of 53.0 wt.% ethylene, 41.0 wt.% propylene and 6.0 wt.% ENB. This material is similar to the product BUNAR® EP G 9650 of the Lanxess Company [55]. This same material was previously studied by Tan et al. [42,45,46] in PEM fuel cell environment.

(5) Fluoroelastomer copolymer (FKM) is a special purpose fluorocarbon-based synthetic rubber. It has wide chemical resistance and superior performance, especially in high temperature application in different media [56]. It's ingredient consists of 1-propene,1,1,2,3,3,3-hexafluoro-, polymer with 1,1-difluoroethene, phosphonium, tributy-2-propenyl-, chloride, phenol,4,4′-[2,2,2-trifluoro-1-(trifluoro-methyl)ethylidene]bis-, carbon black, calcium hydroxide, magnesium oxide, and calcium oxide. This material is similar to the product Viton® fluoroelastomer VTR-9143 of the DuPont Company [57].

Two solutions were used to age the five materials. The first is an accelerated durability test (ADT) solution which is used for short-term, accelerated aging of the material. It consists of 48% HF and 98% H_2SO_4 dissolved in reagent grade water. The final composition is 1 M H_2SO_4, 10 ppm HF and reagent grade water having 18 MΩ resistances. The pH value is less than one. The experiment assumed the ADT solution accelerates chemically the degradation of the five

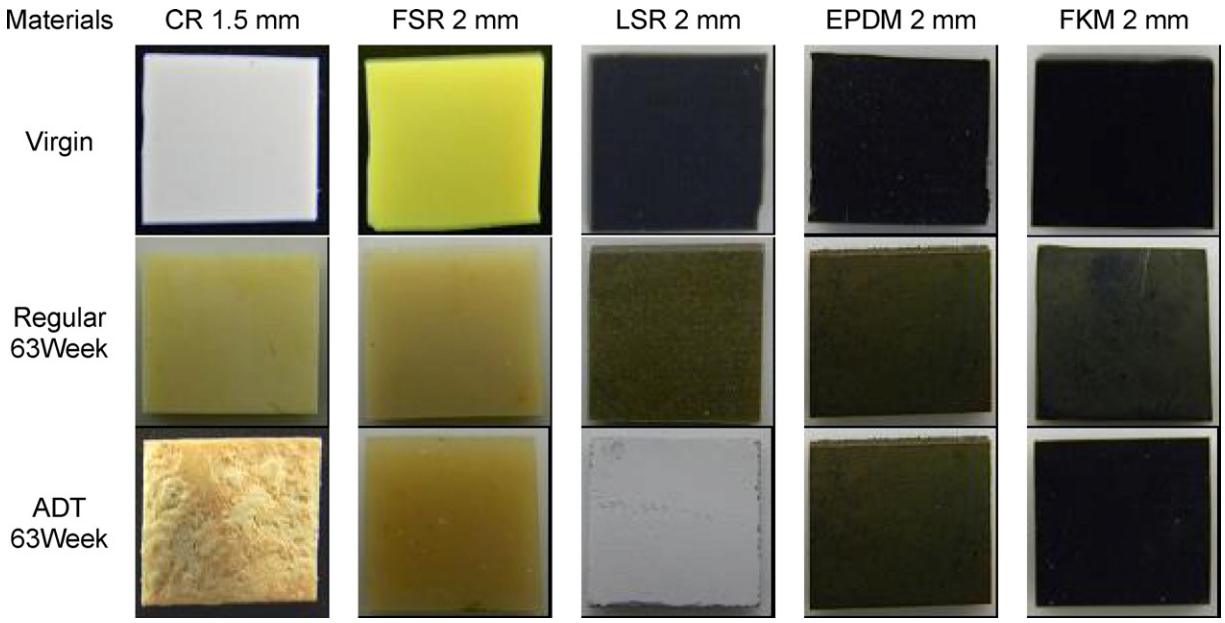

Fig. 1. The sample surface aged in two solutions at 80 °C after 63 week.

materials, but did not alter the degradation mechanism beyond that observed in operating fuel cells. The aging temperature was selected at 80 °C which is close to the operating temperatures of actual PEM fuel cells.

The second solution is termed a "Regular" solution. Chemical composition of the solution is 12 ppm H_2SO_4 and 1.8 ppm HF with reagent grade water having 18 MΩ resistances. The final solution has a pH value of 3.35 which is close to real PEM fuel cell environment. Again, 80 °C was selected to age the materials.

2.2. Characterization methods

Rectangular-shaped specimens were prepared and exposed to either the ADT or the Regular solution. The dimensions of the specimens are 70 mm in length, 20 mm in width, and 2.0 mm in thickness, except copolymeric resin (CR) which has a thickness of 1.5 mm. The samples were submerged in the ADT and Regular solutions in different bottles placed in an oven at a temperature of 80 °C. The aged samples were taken out of the test bottles at selected times for observation and tests. The entire process and tests completed in 63 weeks.

The surface conditions of the virgin and aged samples were observed using optical microscope (Leco, OLYMPUS PME-3) and/or scanning electron microscope (SEM-FEI Quanta 200 Environmental Scanning Electron Microscope). The micro-weight balance (DHAVS E01140) was use to measure the weight change of the test samples. It has a resolution of 0.1 mg. Leachants in the soaking solution was detected using atomic absorption spectrometry (Perkin Elmer 3300) on a regular basis.

ATR-FTIR spectroscopy was performed on the surface of the aged samples using a Nexus Model 670 Instrument (Nicolet Instrument Corporation) and run with 128 scans at a resolution of 4 cm^{-1}. The infrared radiation (IR) penetrates the surface of the test sample to approximately 1 μm. Note that in order to avoid the effect of the remaining ADT and Regular solution on the sample surface on the ATR-FTIR result, the surface of the samples was cleaned using reagent grade water having 18 MΩ resistances to remove the excess of free acids and made dry at room temperature before the ATR-FTIR analysis.

3. Results and discussions

3.1. Surface observation

The surface conditions of the samples were examined before and after exposure to the solutions. The samples were taken out from the test chamber at selected times. After cleaning with reagent grade water, the specimen was placed on paper tower under the chemical hood for four hours at room temperature to let it dry. Fig. 1 shows the virgin sample surface and those after 63 week exposure to the aging solutions. The actual sample size shown in the pictures is about 13 mm by 10 mm.

It can be seen that the colors from the surfaces of CR, FSR and LSR specimen changed after 63 weeks in the 80 °C ADT solution. The color change was most severe for CR and LSR. In addition, there are white powder crystals formed on the surface of CR.

All five materials aged in the Regular solution had color change, while the black color of EPDM and FKM faded only slightly.

3.2. Weight loss

Weight loss of the materials was studied to reveal any erosion of the material by the soaking solution. The samples were taken out from the test chamber at selected times. The surface of the sample was carefully cleaned using reagent grade water having 18 MΩ resistance to remove the excess acids and let dry at room temperature before the weight change was monitored. The percent weight change was calculated using the following equation:

$$\text{Weight change}\,(\%) = \frac{W_2 - W_1}{W_1} \times 100 \quad (1)$$

where W_1 (W_2) is the weight of the sample before (after) aging.

Fig. 2 shows the change of weight over time from the five materials in the two solutions. In general there are three distinct groups – one gained weight, another stayed the same, and one lost weight.

EPDM and FKM gained weight gradually with time in the Regular solution while they remain about the same weight in the ADT solution. The weight gain for both EPDM and FKM in the Regular solution after 63 weeks is about 20%. The reason for this weight gain is explained in the next section.

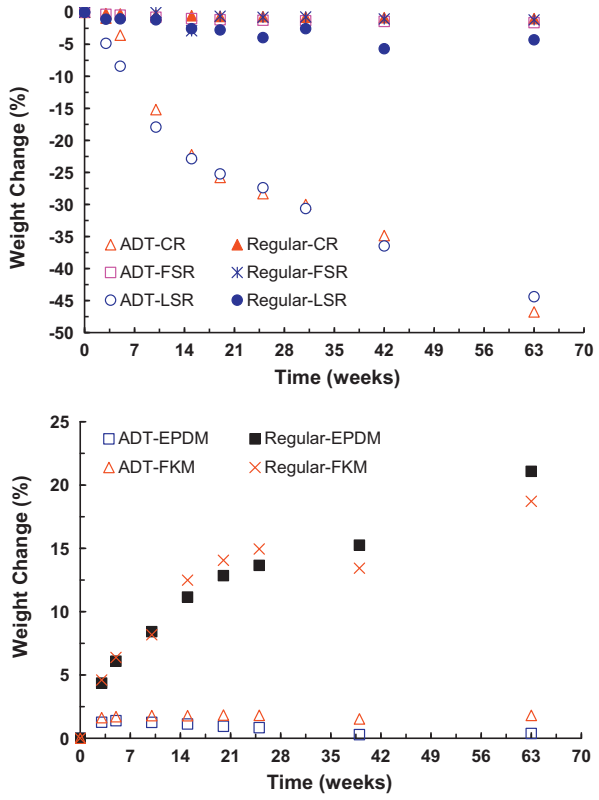

Fig. 2. The weight change of the five materials over time in Regular and ADT solutions.

CR and LSR lost weights gradually in the ADT solution, but not in the Regular solution. Higher concentration of the acid in ADT solution apparently corrodes more out of the material. The weight loss for CR and LSR is about 45% after 63 weeks in the ADT solution.

Overall, both solutions seem to have little effect to the weight of FSR, which outstands itself as the best material in this weight loss study among the five materials. EPDM and FKM gained weight gradually with time in the Regular solution (see Fig. 2), but CR and LSR lost weight in the ADT solution. The results were somewhat consistent with our previous studies on LSR and EPDM, although the test conditions are not exactly identical.

3.3. Optical microscopy

Optical microscopy was used to visually observe the degradation of the surface of the materials in our study. Scales of 50× and 500× are used. Fig. 3 shows that surface conditions of the five materials before and after submerged in the two solutions at 80 °C for 63 weeks. In general, all materials showed some forms of degradation on the surface as fading of the color or/and micro-cracks. Note that cracks can initiate at surface and then propagate through gasket thickness, leading to rupture (particularly under mechanical load/stresses).

The surface conditions of CR, FSR, and LSR changed over time from initially smooth to rough and then cracked. Note that this group of materials also had weight loss as shown in Fig. 2.

The CR material was corroded more in the ADT solution than that in Regular solution. There are micro-cracks formed on the surface of the aged specimens. It appears that small cracks first formed on the surface, its size increased with time, and eventually the sample turned into colored on the surface and cracks became visible after 63 weeks. Additionally, the cracks are apparently deeper in the ADT solution than those in the Regular solution. Fig. 4 shows enlarged view through SEM. Both the powders on the surface and the cracks can be identified easily.

The FSR material also showed surface degradation. However, the surface in Regular solution is smoother compared with virgin material (see 500× in Fig. 3); but rougher in ADT. This is consistent with the weight loss data shown in Fig. 2 where the sample in Regular solution had less weight loss than that in ADT solution

The surface conditions of the LSR samples were also changed over time from initially smooth to rough and the color were changed from slate gray to white. In Fig. 3, one can see that the surface of LSR at 50x in the Regular solution was rougher than that in the ADT solution, but weight loss in the Regular solution (shown in Fig. 2) was less than that in the ADT solution. Fig. 5 shows the SEM pictures of LSR from the edge of the sample soaked in ADT solution. Cracks can be seen in Fig. 5.

In the second group of materials (EPDM, FKM), which had weight gain (see Fig. 2), the optical micrographs in Fig. 3 again show that surface conditions were changed from initially smooth to rough and micro-cracks. FKM had more degradation activities than EPDM. There are crystals formed on the surface of this group of the samples (see a more detailed view in Fig. 6 for EPDM). These crystals are very likely $MgSo_4$. Furthermore, it appears that thicker layer or more crystals are on samples in Regular solution than in ADT. The crystals formed on the sample surface apparently added weight to the sample as reflected in Fig. 2.

It is concluded from this study that (a) the two aging solutions etched out CR, FSR, and LSR materials, (b) ADT solution eroded FSR material, (c) ADT corrodes more materials than the Regular solution, (d) the surface of the aged EPDM was smoother than aged FKM materials, (e) both solutions were corrosive to EPDM materials, (f) there are more chemical activities for FKM than EPDM material in Regular solution; and (g) in general the degradation of the materials can be attributed to the temperature and exposure to the solutions. Similar conclusions were reported earlier for LSR [42–44,47,48] and EPDM [42,45,46].

3.4. Atomic absorption spectrometry

Fillers are required to enhance the mechanical properties, e.g. tensile strength, hardness, and resistance to compression set, of elastomeric materials for gasket or sealing applications. Some of the filler materials such as silicon dioxide and calcium carbonate could be attacked by the simulated PEM fuel cell solutions. Consequently, silicon, calcium and magnesium from the seals could leach out into the soaking solution. To identify the leachants, the atomic absorption spectrometry was employed to analyze the two solutions. Our focus of this part of the work is on the silicon, calcium, and magnesium molecules in the soaking solution that could be detrimental to the electro-chemical operation of PEMFC.

For the chemistries of the five materials studied (see Section 2.1), we anticipated silicon from CR, FSR, and LSR; calcium from LSR, EPDM, and FKM; and magnesium from LSR, EPDM and FKM. The amount of leachant was not known before the tests.

Fig. 7 shows the silicon detected in the two solutions from the five materials over a 63 week span. It is shown that LSR in the Regular solution and CR and LSR in the ADT solution have considerable silicon leachant. This is consistent with the weight loss data shown in Fig. 2. It appears that the severe weight loss of CR and LSR in the ADT solution is attributed to the significant leaching of the silicon.

Both EPDM and FKM do not contain silicon (see Section 2.1) and therefore the nearly zero silicon leachant in either solution shown in Fig. 7 is expected. Among the other three silicon based materials, CR, FSR and LSR, FSR is the only material which has very small amount of silicon leachant in either solution. This is also consistent with the weight loss data shown in Fig. 2, where nearly no change of weight for FSR was observed over the test period.

Fig. 8 shows the calcium leached from the five materials in the two solutions over a 63 week span. LSR is the only material which showed sizable calcium in either ADT or Regular solutions with much higher concentration in ADT. The calcium contents from the other four materials are all small and less than 1 mg L^{-1}.

The magnesium results are shown in Fig. 9. The quantitative amount of magnesium found in the solutions is very small, e.g. all less than 1 mg L^{-1}, compared to silicon and calcium. The three highest concentration cases in rank order are: LSR in ADT, FKM in Regular and EPDM in Regular solution. Again, similar to the weight loss, the behavior of EPDM and FKM in Regular solution appears to be more active than that in ADT, despite that ADT is more acidic.

Comparing the three leachants, silicon has much higher concentrations than calcium or magnesium (see the scale of the ordinate in Figs. 7–9). This is particularly true for LSR as it is a silicon based material. Similar results for LSR and EPDM were reported by Tan et al. [42] although the test designs were somewhat different.

3.5. Attenuated total reflection-Fourier transform infrared (ATR-FTIR) analysis

ATR-FTIR analysis was used to determine any chemistry changes as an indication of chemical degradation that occurred to the five materials (CR, FSR, LSR, EPDM and FKM) in the simulated PEM fuel cell environment. The spectra for the virgin and aged materials at various exposure times to the two simulated fuel cell environments are presented in this section. We focused our attention in the wavenumbers between 800 cm^{-1} and 4000 cm^{-1}. All results

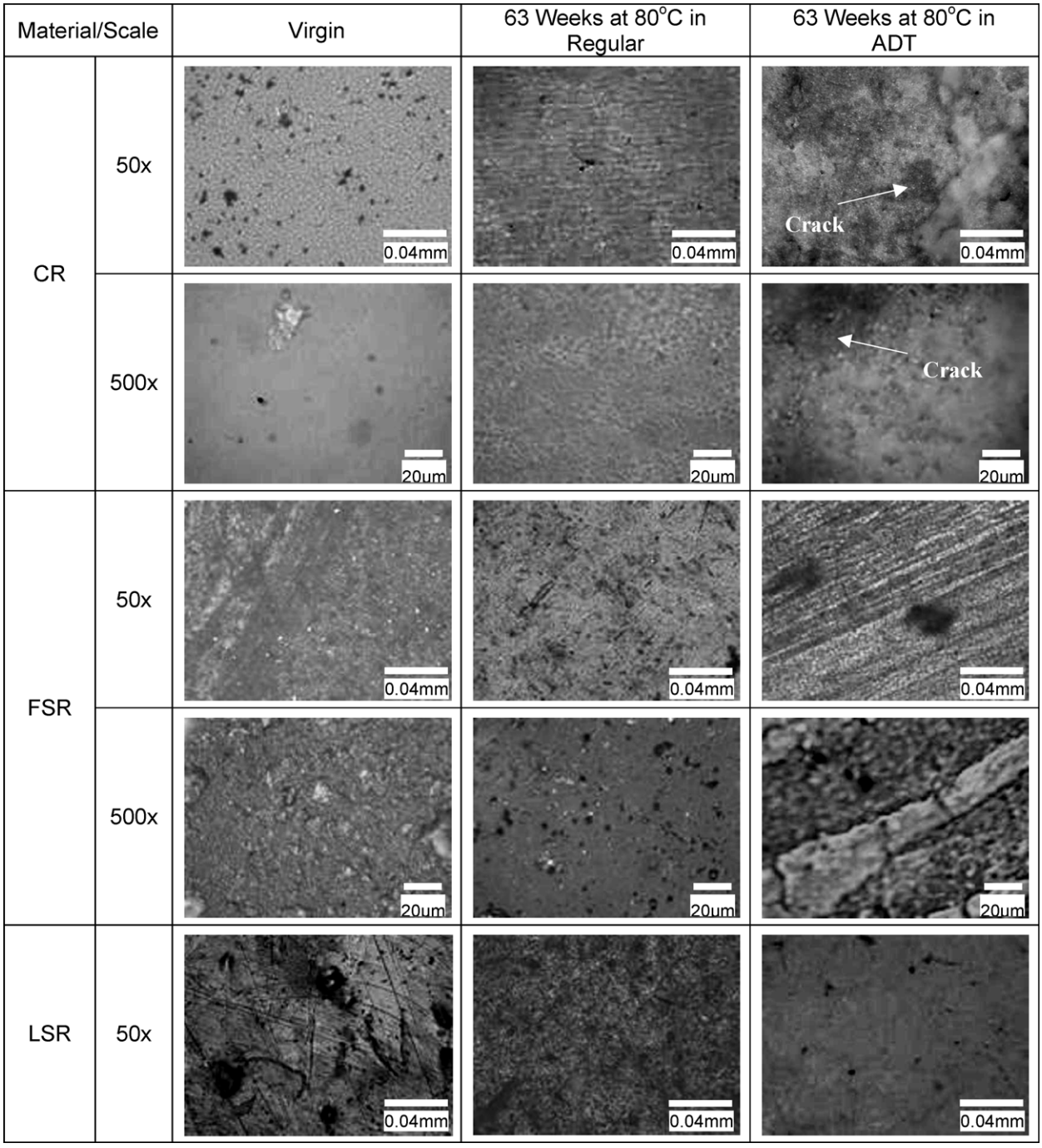

Fig. 3. Specimen surface conditions – virgin and aged 63 weeks in ADT and Regular solution at 80 °C.

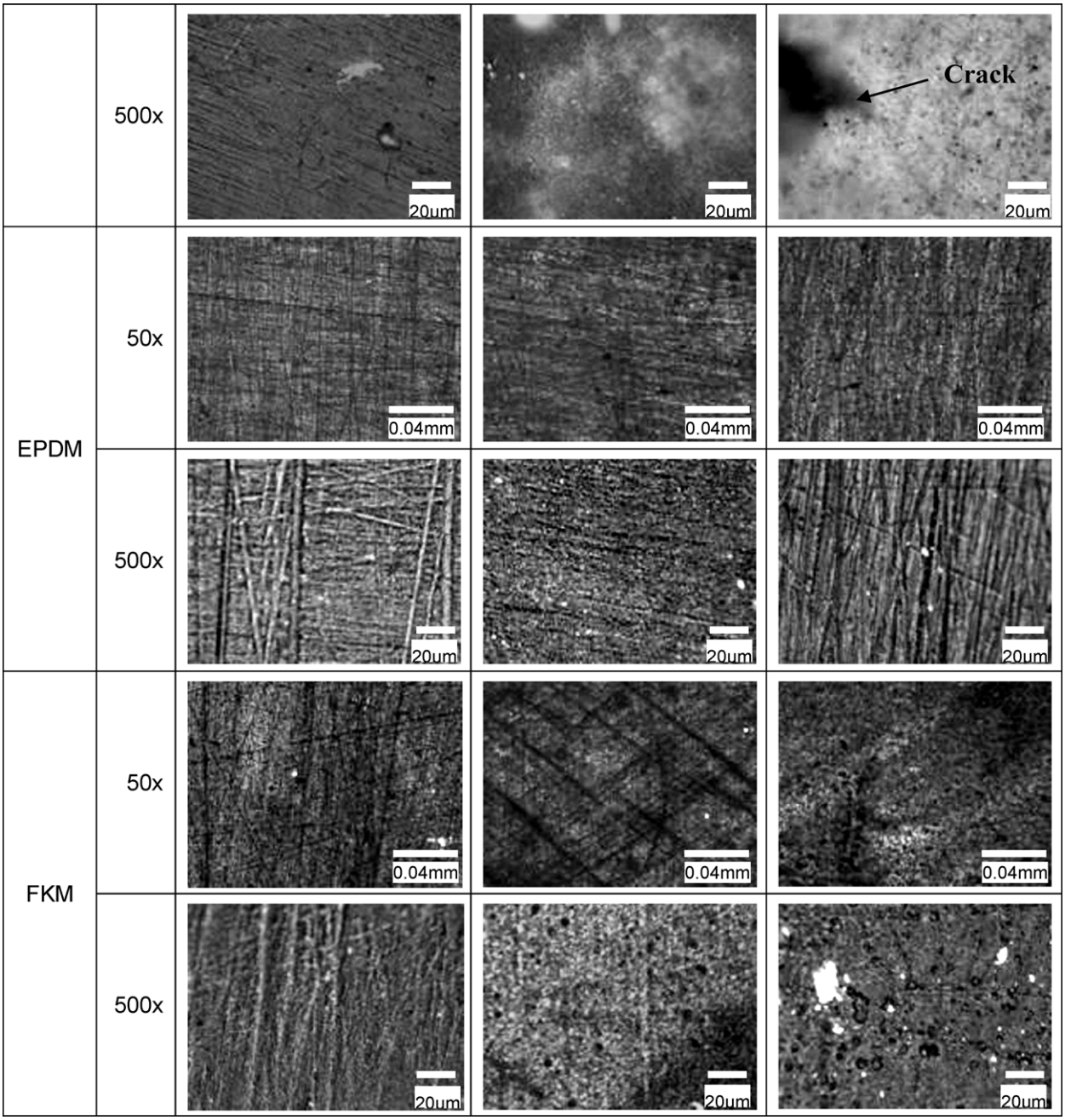

Fig. 3. (*Continued*).

are plotted in two figures, one from 800 cm^{-1} to 1800 cm^{-1} and another from 2800 cm^{-1} to 3200 cm^{-1}, as there is no peak in wavenumbers from 1800 cm^{-1} to 2800 cm^{-1} and from 3200 cm^{-1} to 4000 cm^{-1}. All correspondence between the spectrum and the vibration mode throughout the article was obtained from the handbook by Lin-Vien et al. [58], Colvin [59] and Streiwieser and Heathcock [60].

3.5.1. Copolymeric resin (CR)

Data from ATR-FTIR analysis for the CR samples before and after exposure to the Regular solution at 80 °C at various times up to 63 week are shown in Fig. 10. As shown in Fig. 10(A), the strongest peaks for the unexposed samples are at 1020 cm^{-1} and 1090 cm^{-1} which are from the stretching vibrations of Si–O–Si present in this material. The peaks at 1260 cm^{-1} and 866 cm^{-1} are from the bending vibration of $Si–CH_3$ and the rocking vibration of $Si–CH_3$, respectively. The peaks at 2960 cm^{-1} are from the stretching vibration mode of CH_3. The peaks near 1418 cm^{-1} are from the rocking vibration of $–CH_2–$ as a part of the CR crosslinked domain. The peak at 1150 cm^{-1} is the stretching vibration of C–O–C or from the skeletal vibration mode of C–C. The peak at 1210 cm^{-1} is from the stretching vibration of ν(Si–O–Si) and 1260 cm^{-1} is due to $\delta(Si–CH_3)$ bending mode.

In Fig. 11, FTIR data for CR material in the ADT solution over a 63 week period was presented. As shown in the Fig. 11(A), the intensity of the peaks between 1020 cm^{-1} and 1090 cm^{-1} decreased with time which is consistent with the previous results [42–44]. The drop of the intensity is more than that in the Regular solution. The peaks at 866 cm^{-1}, 1210 cm^{-1}, and 1418 cm^{-1} as shown in Fig. 11(A) and at 2960 cm^{-1} in Fig. 11(B) decreased sharply after exposure to the solution and then almost disappeared after 3-week exposure to the ADT solution at 80 °C.

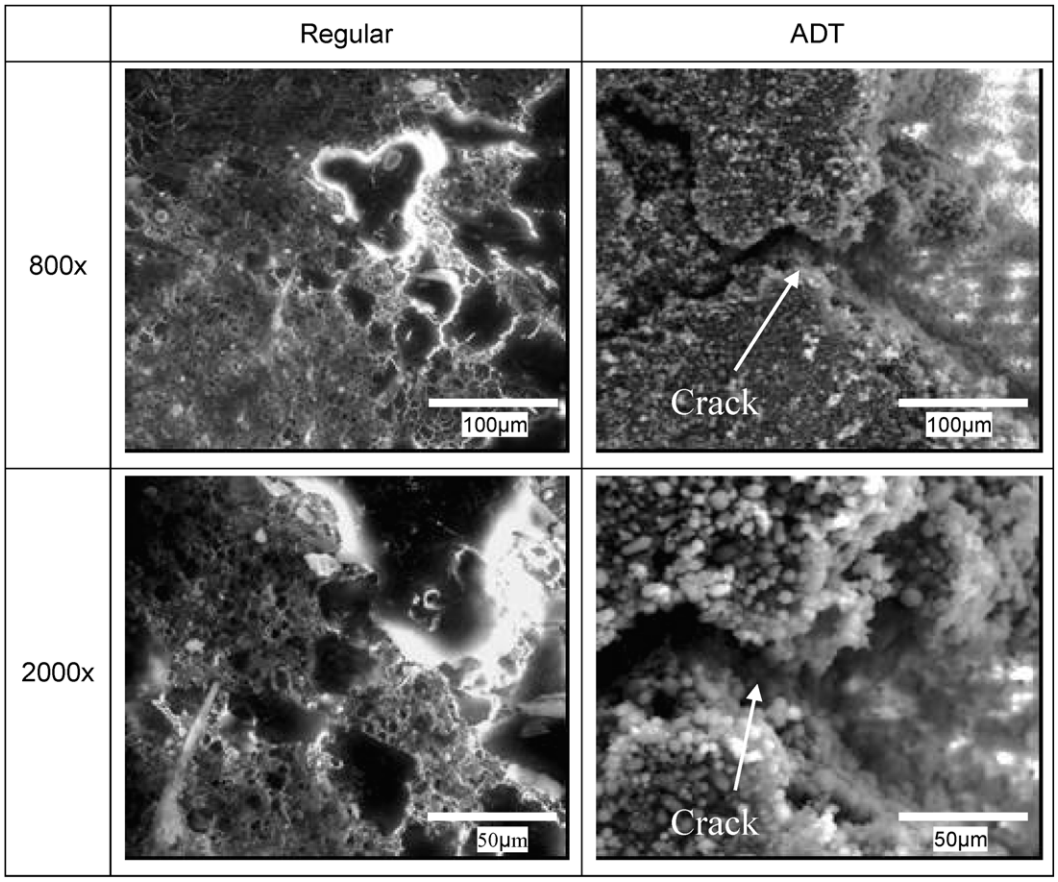

Fig. 4. SEM surface conditions of CR specimens– aged after 63 weeks in the two solutions at 80 °C.

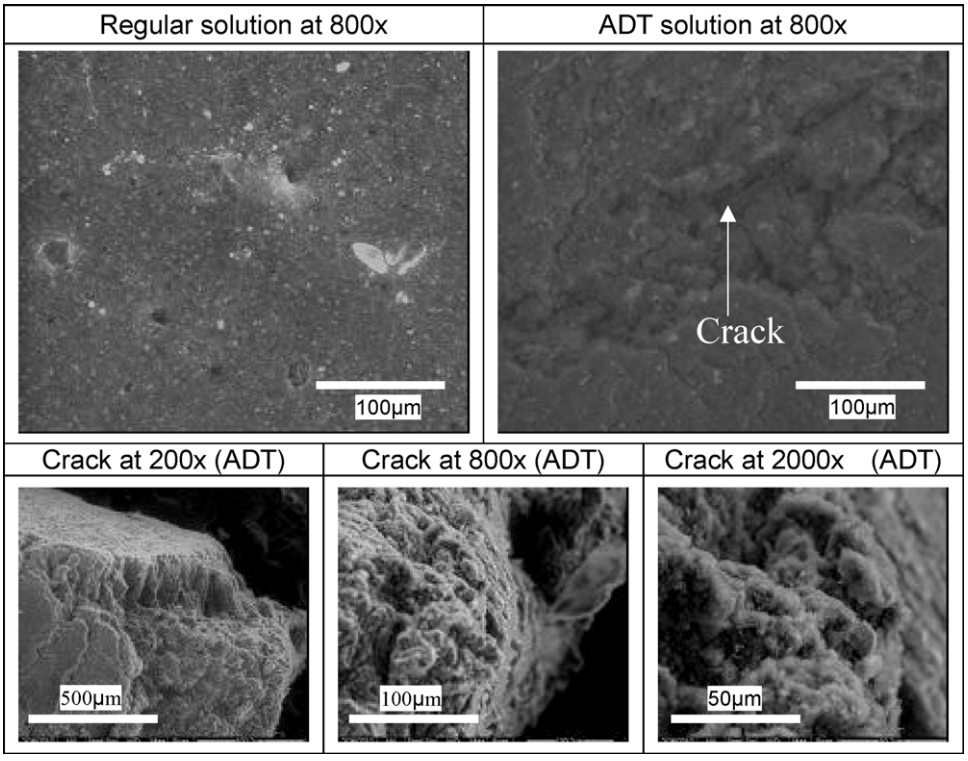

Fig. 5. SEM surface conditions of LSR specimens– aged after 63 weeks in the two solutions at 80 °C.

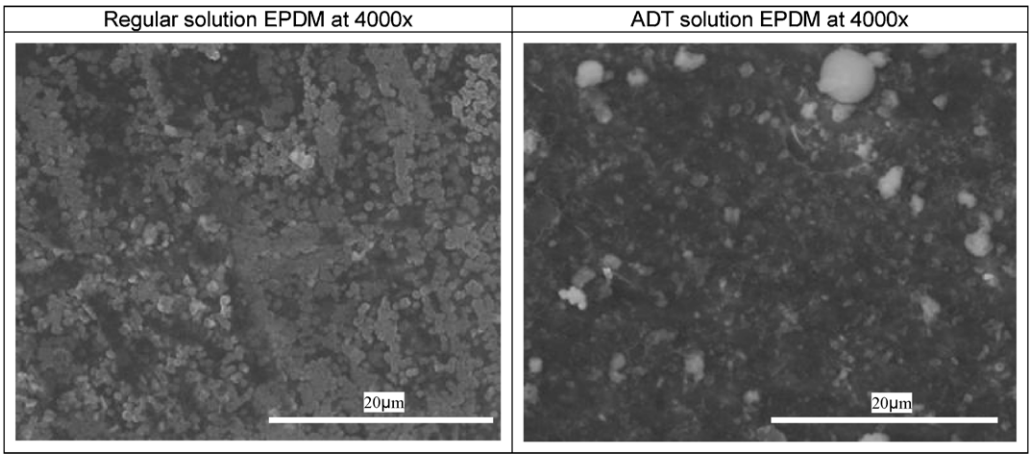

Fig. 6. Enlarged view of EPDM sample showing the crystals formed on the surface – more crystals in regular than in ADT solution.

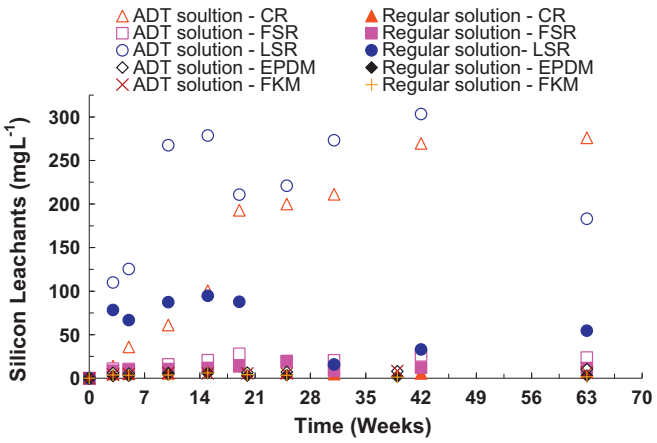

Fig. 7. Silicon leached from the five materials in two solutions over 63 weeks at 80 °C.

The extent of decrease of the intensity at 866 cm^{-1}, 1260 cm^{-1}, 1418 cm^{-1}, and 2960 cm^{-1} is slightly more than that in Regular solution under identical conditions.

Comparing CR results of the FTIR data from the two solutions, the degradation mechanisms of the material is similar except that the extent of degradation in ADT solution is more severe than that in Regular solution. It may be concluded that CR material in Regular solution is more chemically stable than in ADT solution under current test conditions.

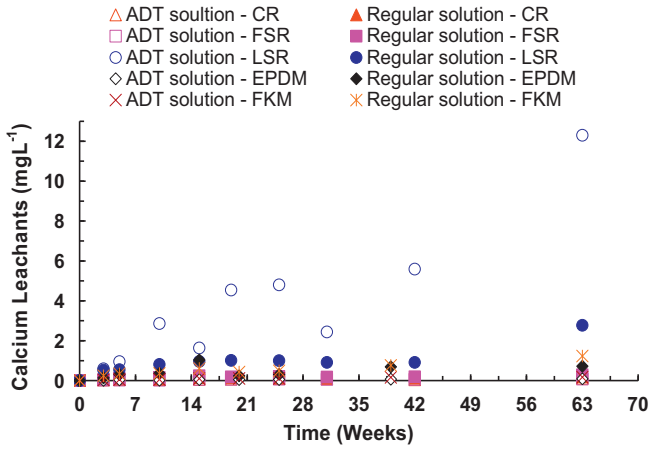

Fig. 8. Calcium leached from the five materials in two solutions over time at 80 °C.

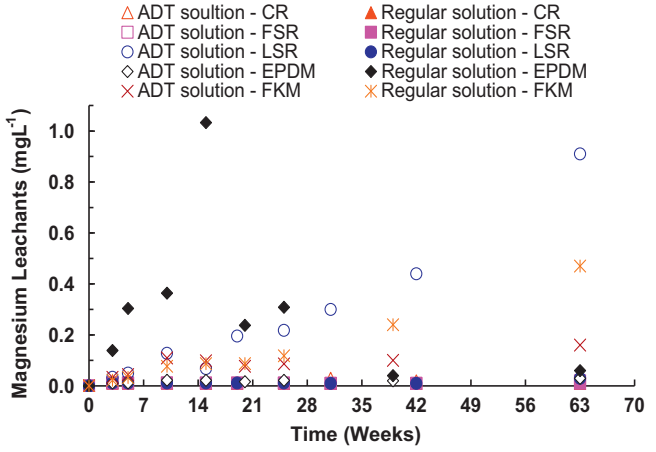

Fig. 9. Magnesium leached from the five materials in two solutions over time at 80 °C.

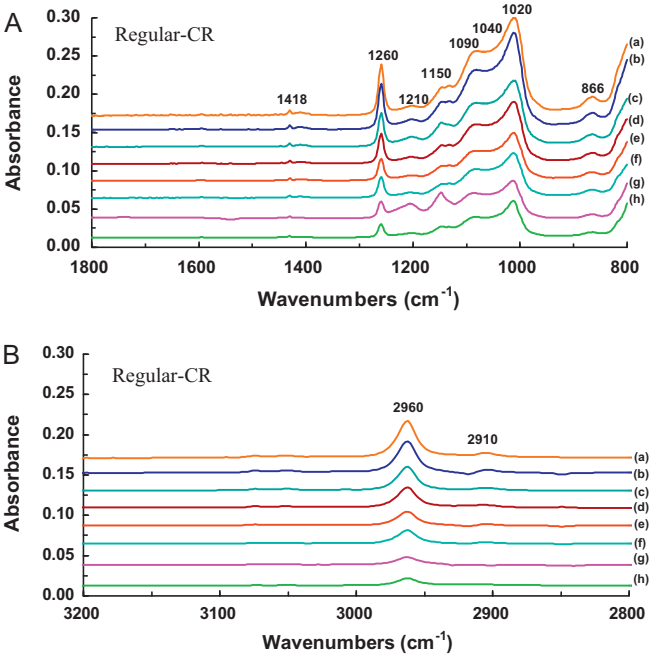

Fig. 10. ATR-FTIR results for CR material before, after, and up to 63 week exposure to Regular solution at 80 °C – (A) wave numbers from 800 cm^{-1} to 1800 cm^{-1}; (B) wave numbers from 1800 cm^{-1} to 3200 cm^{-1}; (a) 0 week, (b) 3 week, (c) 5 week, (d) 10 week, (e) 15 week, (f) 19 week, (g) 42 week, (h) 63 week exposure.

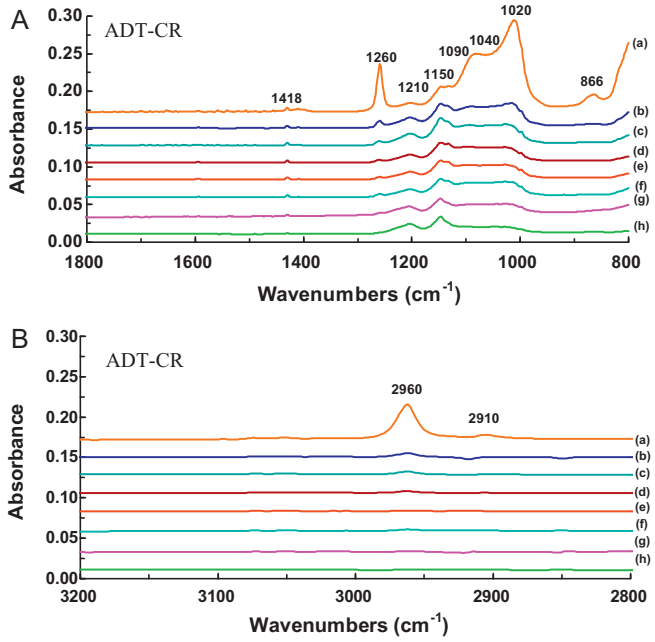

Fig. 11. ATR-FTIR results for CR material before, after, and up to 63 week exposure to ADT solution at 80 °C – (A) wave numbers from 800 cm^{-1} to 1800 cm^{-1}; (B) wave numbers from 1800 cm^{-1} to 3200 cm^{-1}; (a) 0 week, (b) 3 week, (c) 5 week, (d) 10 week, (e) 15 week, (f) 19 week, (g) 42 week, (h) 63 week exposure.

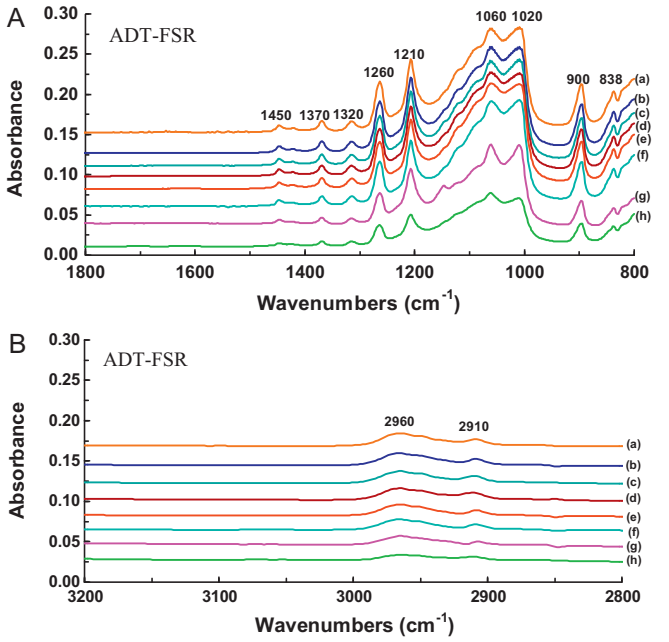

Fig. 13. ATR-FTIR results for FSR material before, after, and up to 63 week exposure to ADT solution at 80 °C – (A) wavenumbers from 800 cm^{-1} to 1800 cm^{-1}; (B) wavenumbers from 1800 cm^{-1} to 3200 cm^{-1}; (a) 0 week, (b) 3 week, (c) 5 week, (d) 10 week, (e) 15 week, (f) 19 week, (g) 42 week, (h) 63 week exposure.

3.5.2. *Fluorosilicone rubber (FSR)*

ATR-FTIR results for FSR in Regular solution at 80 °C are plotted in Fig. 12. The peaks are at 838 cm^{-1}, 900 cm^{-1}, 1020 cm^{-1}, 1060 cm^{-1}, 1210 cm^{-1}, 1260 cm^{-1}, 1320 cm^{-1}, 1370 cm^{-1}, and 1450 cm^{-1} shown in Fig. 12(A) and at 2910 cm^{-1} and 2960 cm^{-1} in Fig. 12(B). The stronger peaks were at wavenumbers 900 cm^{-1}, 1020 cm^{-1}, 1060 cm^{-1}, 1210 cm^{-1} and 1260 cm^{-1}.

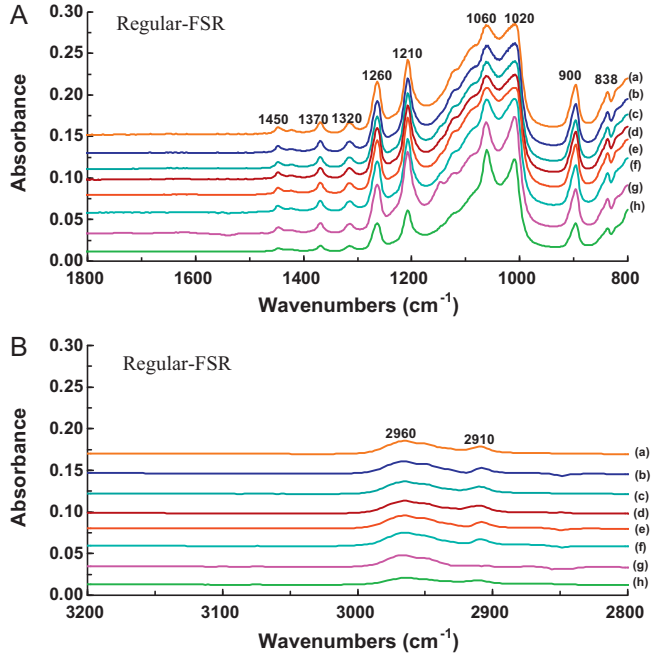

Fig. 12. ATR-FTIR results for FSR material before, after, and up to 63 week exposure to Regular solution at 80 °C – (A) wave numbers from 800 cm^{-1} to 1800 cm^{-1}; (B) wave numbers from 1800 cm^{-1} to 3200 cm^{-1}; (a) 0 week, (b) 3 week, (c) 5 week, (d) 10 week, (e) 15 week, (f) 19 week, (g) 42 week, (h) 63 week exposure.

The strongest and broadest peaks for the unexposed samples are between 1020 cm^{-1} and 1060 cm^{-1} which are from the stretching vibrations of Si–O–Si in this material. The peak at 1210 cm^{-1} is from the stretching vibration of ν(Si–O–Si) and at 1260 cm^{-1} is due to $\delta(Si–CH_3)$ bending vibration mode. The peak at 838 cm^{-1} is from C–H bending. The wavenumber at 900 cm^{-1} is Si–F [61]. The peaks near 1320 cm^{-1}, 1370 cm^{-1} and 1450 cm^{-1} are from the S=O vibration mode [62]. The weakest peaks among these are 2910 cm^{-1} and 2960 cm^{-1} from the stretching vibrations of CH_3.

In Fig. 13, FTIR results for FSR material in the ADT solution were presented. Essentially no FTIR spectrum changes were observed for FSR in either Regular or ADT solutions.

3.5.3. *Liquid silicone rubber (LSR)*

Figs. 14 and 15 show the ATR-FTIR results for the LSR material before, after, and up to 63 week exposure to the Regular and ADT solution, respectively, at 80 °C. In the Regular solution, the strongest peaks for the unexposed samples are at 866 cm^{-1}, 1020 cm^{-1}, 1040 cm^{-1}, 1090 cm^{-1}, 1150 cm^{-1}, 1210 cm^{-1}, 1260 cm^{-1}, 1418 cm^{-1} (see Fig. 14(A)) and at 2910 cm^{-1} and 2960 cm^{-1} (see Fig. 14(B)). The peak at wavenumber 866 cm^{-1} is due to $\rho(Si–CH_3)$ rocking vibration, and at 1260 cm^{-1} is due to $\delta(Si–CH_3)$ bending mode. The peaks at 1020 cm^{-1}, 1040 cm^{-1}, 1090 cm^{-1}, and 1210 cm^{-1} are from the stretching vibrations of ν(Si–O–Si). The peak at 1150 cm^{-1} is from the stretching vibration of C–O–C or from the skeletal vibration mode of C–C. The peaks near 1418 cm^{-1} are from the rocking vibration of $–CH_2–$, and at 2910 cm^{-1} and 2960 cm^{-1} are from the stretching vibration mode of CH_3.

After 42 weeks, the peaks at wavenumbers 1418 cm^{-1}, 2910 cm^{-1} and 2960 cm^{-1} disappeared in Regular solution (see Fig. 14(A) and (B)). It is most likely due to the damage of the CH through the hydrolysis to form OH.

The peaks at 866 cm^{-1}, 1020 cm^{-1}, 1040 cm^{-1}, 1260 cm^{-1} and 1418 cm^{-1} disappeared immediately after 3 weeks in the ADT solution (see Fig. 15(A)). So did those at 2910 cm^{-1} and 2960 cm^{-1} (see Fig. 15(B)). That means the ADT solution and temperature had accel-

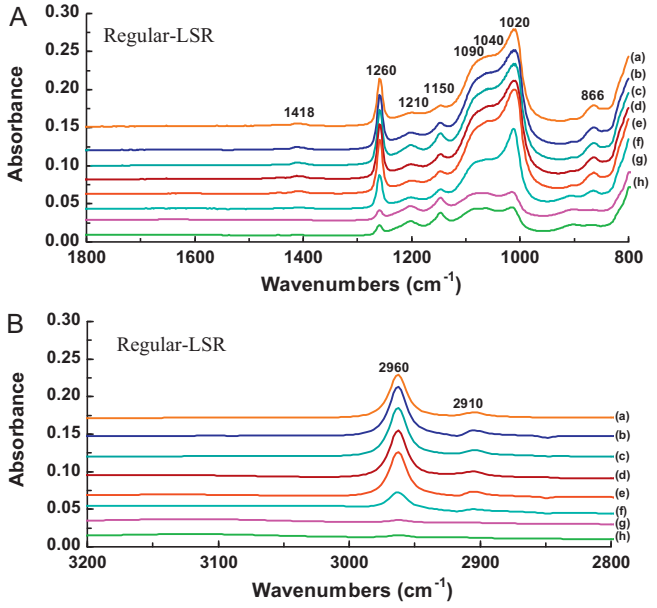

Fig. 14. ATR-FTIR results for LSR material before, after, and up to 63 week exposure to Regular solution at 80 °C – (A) wavenumbers from 800 cm^{-1} to 1800 cm^{-1}; (B) wavenumbers from 1800 cm^{-1} to 3200 cm^{-1}; (a) 0 week, (b) 3 week, (c) 5 week, (d) 10 week, (e) 15 week, (f) 19 week, (g) 42 week, (h) 63 week exposure.

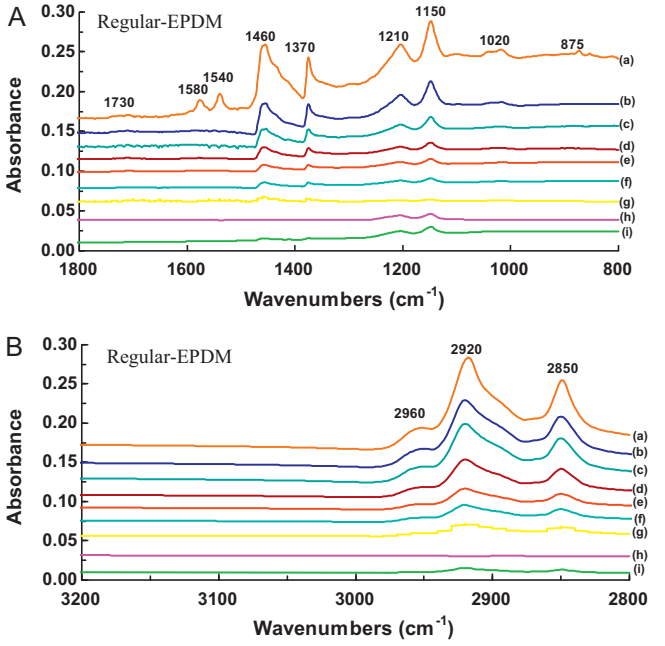

Fig. 16. ATR-FTIR results for EPDM material before, after, and up to 63 week exposure to Regular solution at 80 °C – (A) wavenumbers from 800 cm^{-1} to 1800 cm^{-1}; (B) wavenumbers from 1800 cm^{-1} to 3200 cm^{-1}; (a) 0 week, (b) 3 week, (c) 5 week, (d) 10 week, (e) 15 week, (f) 19 week, (g) 42 week, (h) 63 week exposure.

erated dissolving reaction to LSR. These decreases in the intensity of the peaks in the silicone rubber crosslinked domain is most likely due to the damage of the Si–C through the hydrolysis to form Si–OH [43].

It is concluded that there are significant chemical changes for samples exposed to ADT solution at 80 °C over time. It is believed that the chemical degradation is likely due to de-crosslinking and chain scissoring in the rubber backbone in the environment. This conclusion is consistent to our previous results in [42–44,48].

3.5.4. Ethylene propylene diene monomer rubber (EPDM)

Figs. 16 and 17 present the FTIR results for EPDM in Regular and ADT solution, respectively. The FTIR spectrum for the virgin EPDM shows that the strongest and broadest peaks are at 1150 cm^{-1}, 1370 cm^{-1}, 1460 cm^{-1}, 2850 cm^{-1} (see Figs. 16(A) and 17(A)) and at 2920 cm^{-1} (see Figs. 16(B) and 17(B)). The peaks at wavenumbers 2850–3000 cm^{-1} are from CH_3, CH_2 and CH. And, at 1150 cm^{-1} is from the stretching vibration mode of C–O–C or from the skeletal vibration mode of C–C. The peak at 1210 cm^{-1} is from the stretch-

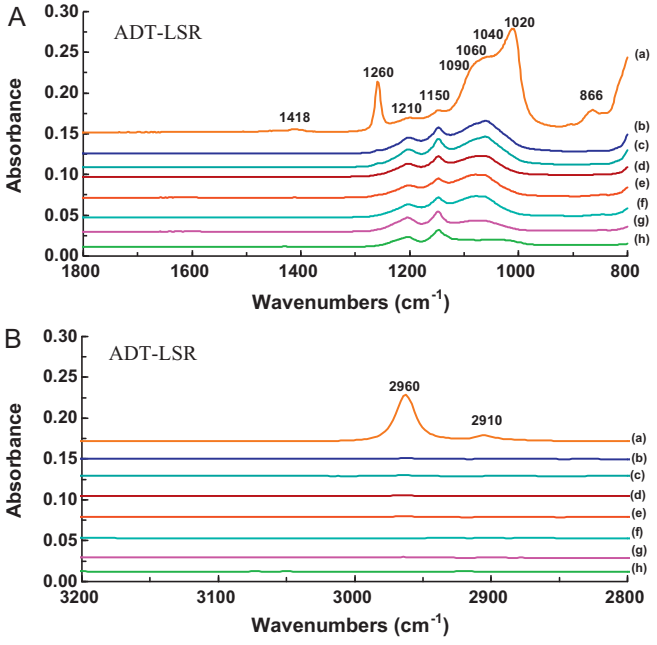

Fig. 15. ATR-FTIR results for LSR material before, after, and up to 63 week exposure to ADT solution at 80 °C – (A) wavenumbers from 800 cm^{-1} to 1800 cm^{-1}; (B) wavenumbers from 1800 cm^{-1} to 3200 cm^{-1}; (a) 0 week, (b) 3 week, (c) 5 week, (d) 10 week, (e) 15 week, (f) 19 week, (g) 42 week, (h) 63 week exposure.

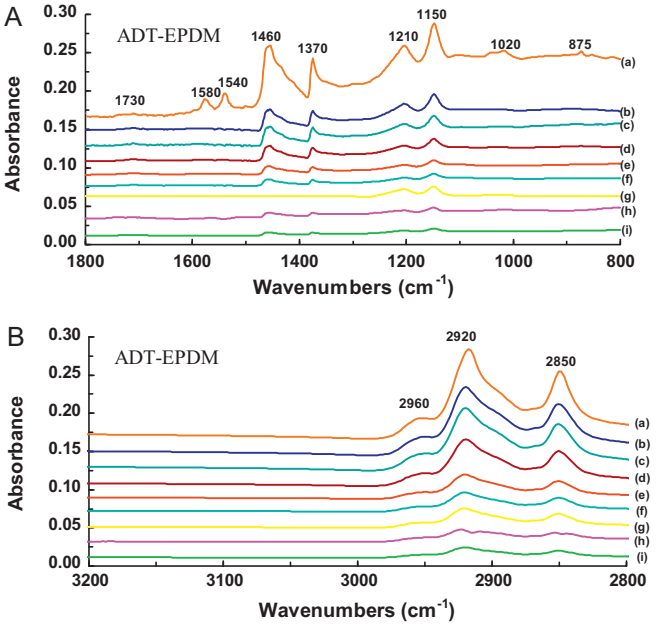

Fig. 17. ATR-FTIR results for EPDM material before, after, and up to 63 week exposure to ADT solution at 80 °C – (A) wavenumbers from 800 cm^{-1} to 1800 cm^{-1}; (B) wavenumbers from 1800 cm^{-1} to 3200 cm^{-1}; (a) 0 week, (b) 3 week, (c) 5 week, (d) 10 week, (e) 15 week, (f) 19 week, (g) 42 week, (h) 63 week exposure.

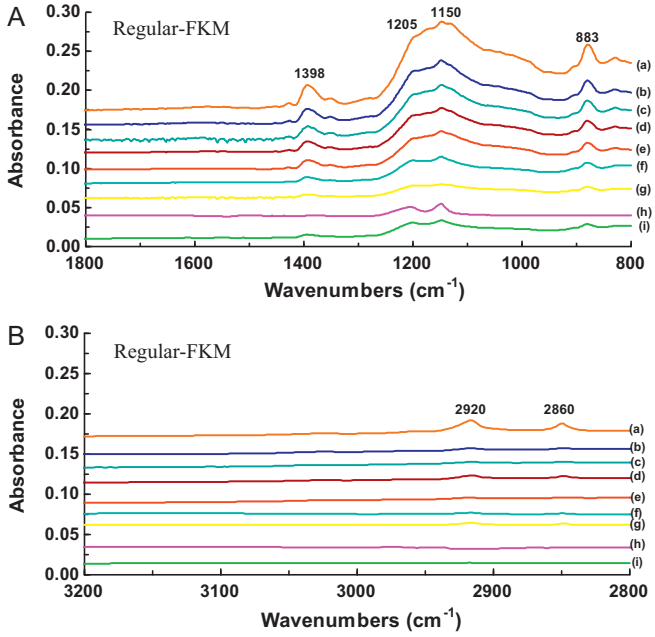

Fig. 18. ATR-FTIR results for FKM material before, after, and up to 63 week exposure to Regular solution at 80 °C – (A) wavenumbers from 800 cm^{-1} to 1800 cm^{-1}; (B) wavenumbers from 1800 cm^{-1} to 3200 cm^{-1}; (a) 0 week, (b) 3 week, (c) 5 week, (d) 10 week, (e) 15 week, (f) 19 week, (g) 42 week, (h) 63 week exposure.

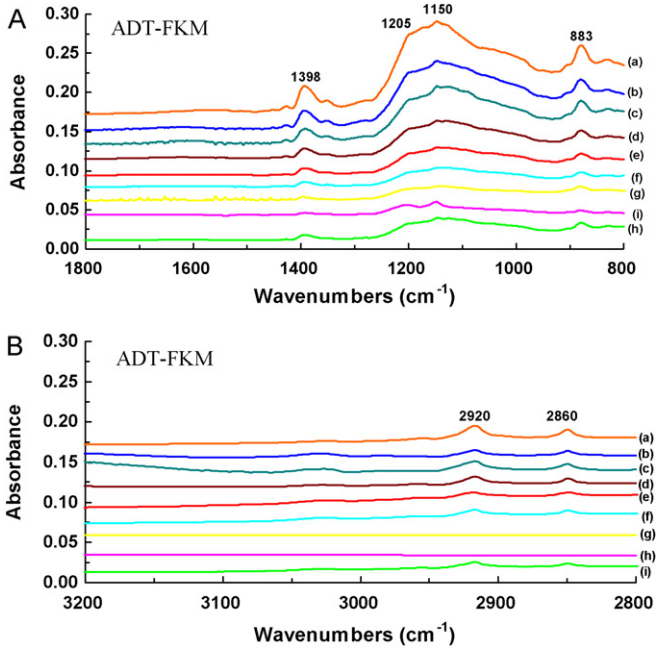

Fig. 19. ATR-FTIR results for FKM material before, after, and up to 63 week exposure to ADT solution at 80 °C – (A) wavenumbers from 800 cm^{-1} to 1800 cm^{-1}; (B) wavenumbers from 1800 cm^{-1} to 3200 cm^{-1}; (a) 0 week, (b) 3 week, (c) 5 week, (d) 10 week, (e) 15 week, (f) 19 week, (g) 42 week, (h) 63 week exposure.

ing vibration of ν(Si–O–Si). The peaks at 1370 cm^{-1} and 1460 cm^{-1} are from the $-CH_2-$ scissoring vibration mode and symmetric C–H stretching mode of CH_3 from the propylene unit of EPDM material, respectively. The peaks at 1540 cm^{-1} 1580 cm^{-1} were from N=O (nitro) [63].

Both the peaks at 1540 cm^{-1} and 1580 cm^{-1} disappeared after 3 weeks. That could be due to carboxylates present on the sample surface, or vulcanization products present on EPDM surface [46].

EPDM rubber has the inherent resistance to heat (up to 120 °C) and acid (for example, 60% sulfuric acid solution or 50% nitric acid solution) [60] due to its saturated hydrocarbon backbone. Although the main chains in EPDM rubber are quite stable, the material can be attacked/damaged in strong acidic environment and this can cause significant chemical changes [20,21,63,64]. The chemical degradation of EPDM rubber depends on the nature and types of the cross-linking as well as the crosslinking density. It also depends on the nature and types of the accelerators as well as the ratios of sulphur to accelerator for the sulphur curing system and the chemical structure of co-agents used in peroxide curing system [63]. The degradation mechanisms could proceed via de-crosslinking through hydrolysis of the crosslinks in addition to the attack by aqueous acid on the C=C of ENB present in the EPDM in a strong acidic environment [20,21,63].

In both solutions, the FTIR results (Figs. 16(A) and 17(A)) show that the peak intensities at wavenumbers 875 cm^{-1}, 1020 cm^{-1}, 1540 cm^{-1}, 1580 cm^{-1}, and 1730 cm^{-1} almost disappeared after 3 week exposure. Comparing the two solutions, the degradation mechanisms are similar except that the rate of degradation is faster in ADT.

3.5.5. *Fluoroelastomer copolymer (FKM)*

FTIR results from FKM are presented in Figs. 18 and 19. The virgin material shows the peaks of intensity at wavenumbers 883 cm^{-1}, 1150 cm^{-1}, 1200 cm^{-1}, 1400 cm^{-1}, 2860 cm^{-1}, and 2920 cm^{-1}.

The intensity peaks in the Regular solution at wavenumbers 2860 cm^{-1} and 2920 cm^{-1} decreased slowly from 3 to 63 weeks (see Fig. 18(B)). The peaks at wavenumbers near 2850–3000 cm^{-1} which are from CH_3, CH_2 and CH disappeared after 63 weeks. The peaks at 883 cm^{-1}, 1205 cm^{-1} and 1398 cm^{-1} are from the synthetic process described previously and resulted in a sol–gel Fe_2O_3 material that decreased after 19 week in both the solutions.

The intensities at the wavenumbers 1400 cm^{-1}, 2860 cm^{-1} and 2920 cm^{-1} gradually decreased in both solutions. It appears that the degradation mechanisms of the FKM material are similar in the two solutions, except that the rate of degradation is faster in ADT.

4. Conclusions

Chemical degradation characteristics of five elastomeric gasket materials, copolymeric resin (CR), fluorosilicone rubber (FSR), liquid silicone rubber (LSR), ethylene propylene diene monomer rubber (EPDM), and fluoroelastomer copolymer (FKM), in a simulated and an accelerated PEM Fuel Cell solution were studied. Under the tests conditions and the test results, the following conclusions can be made:

1. Overall, FSR is the most stable material, followed by EPDM, FKM, LSR and CR in rank order, based on (a) CR, LSR materials had cracks and CR had more surface cracks than LSR, and (b) EPDM had weight gain and the leachants are less than FKM.
2. Observed from the appearance, there are color changes on the surface of the aged materials. CR and LSR in the ADT solution have the most color change. SEM pictures for the CR material showed white powders formed on the surface and small piece peeled off from the surface of the LSR material in the ADT solution. EPDM in either solution showed some erosion.
3. From the weight loss study, it is found (a) CR, LSR had some weight loss, but EPDM and FKM had weight gain, (b) the amount of weight loss or gain monotonically relates to the aging time, and (c) FSR had negligible weight change in both solutions.
4. From the atomic absorption spectrometry analysis, it is found (a) both CR and LSR materials have silicon leached out, (b) LSR has calcium atoms leached out, and (C) LSR, EPDM and FKM have magnesium leached out. FSR had almost no leachant.

5. From the FTIR study, materials in the Regular solution, in general, are more stable than in the ADT solution under the test conditions. The CR and LSR in the ADT solution are not as stable as the other three materials. FSR seems to be the most stable among the five materials studied.

Note that selection of any seal material will be based on chemical and physical performance as well as cost. This paper addresses the chemical stability and therefore all conclusions and rankings are based on chemical stability of the materials only. Physical durability such as stress relaxation and cost (from both the material itself and fabrication) are out of the scope of the current paper and will be addressed elsewhere.

Acknowledgements

This study is sponsored by Graduate Students Research Abroad Program (Grant No. 97-2917-I-110-108) from National Research Council, Taiwan, and National Sun Yat-Sen University Study Abroad Scholarship Award to the first author. In addition, support from the US Department of Energy (DE-FC36-06G086041 and DE-FG36-08GO88116) to the University of South Carolina Research Foundation, the NSF Industry/University Cooperative Research Center for Fuel Cells at the University of South Carolina (EEC-0324260 and IIP-0856055) and, and Natural Science Foundation of Jiangsu Province in China (BK2009362) is greatly appreciated. Materials in this study were kindly provided by Dow-Corning and Dana Corporation. Y.J. Chao also wants to thank the partial support from China 111 project (B08040) awarded to the School of Materials Science, Northwestern Polytechnical University, Xian, China. The authors are indebted to Drs. Rick Blunk (General Motor Corporation), Eve Steigerwalt (Dana), and Peter Lo (Dow-Corning) for their insightful advice and technical discussions.

References

[1] L. Frisch, PEMFC Stack Sealing Using Silicone Elastomers, 2003 SAE World Congress 2003-01-0801, 2003.
[2] S. Kole, K. Srivastava, D.K. Tripathy, A.K. Bhowmick, J. Appl. Polym. Sci. 54 (9) (1994) 1329–1337.
[3] A.K. Bhowmick, J. Konar, S. Kole, S. Narayanan, J. Appl. Polym. Sci. 57 (5) (1995) 631–637.
[4] B.H. Youn, C.S. Huh, IEEE Trans. Dielect. Electr. Insul. 12 (5) (2005) 1015–1024.
[5] J. Konar, G. Samanta, B.N. Avasthi, A.K. Sen, Polym. Degrad. Stab. 43 (2) (1994) 209–216.
[6] T. Zaharescu, M. Giurginca, Proceedings of the 1995 IEEE 5th International Conference on Conduction and Breakdown in Solid Dielectric, Leicester, England, 1995, pp. 472–476.
[7] T. Zaharescu, M. Giurginca, S. Jipa, Polym. Degrad. Stab. 63 (2) (1999) 245–251.
[8] R.A. Assink, M. Celina, K.T. Gillen, R.L. Clough, T.M. Alam, Polym. Degrad. Stab. 73 (2) (2001) 355–362.
[9] T. Zaharescu, E. Feraru, C. Podina, Polym. Degrad. Stab. 87 (1) (2005) 11–16.
[10] A. Ghanbari-Siahkali, S. Mitra, P. Kingshott, K. Almdal, C. Bloch, H.K. Rehmeier, Polym. Degrad. Stab. 90 (3) (2005) 471–480.
[11] A.N. Chaudhry, N.C. Billingham, Polym. Degrad. Stab. 73 (3) (2001) 505–510.
[12] M.A. Kader, A.K. Bhowmick, Thermal Ageing, Polym. Degrad. Stab. 79 (2) (2003) 283–295.
[13] M. Patel, A.R. Skinner, R.S. Maxwell, Polym. Test. 24 (5) (2005) 663–668.
[14] L. Zhang, Z. Xu, Q. Wei, S. He, Radiat. Phys. Chem. 75 (2) (2006) 350–355.
[15] R.L. Hauser, R. Hauser Quick Jr., N. Allen, A.E. Williams, Rubber World 224 (5) (2001) 24–26.
[16] A.U. Paeglis, Rubber Chem. Technol. 77 (2) (2004) 242–256.
[17] M. Ehsani, H. Borsi, E. Gockenbach, G.R. Bakhshandeh, J. Morshedian, Adv. Polym. Technol. 24 (1) (2005) 51–56.
[18] H. Liu, G. Cash, D. Birtwhistle, G. George, IEEE Trans. Dielect. Electr. Insul. 2 (3) (2005) 478–486.
[19] D. Graiver, K.W. Farminer, R. Narayan, J. Polym. Environ. 11 (4) (2003) 129–136.
[20] S. Mitra, A. Ghanbari-Siahkali, P. Kingshott, H.K. Rehmeier, H. Abildgaard, K. Almdal, Polym. Degrad. Stab. 91 (1) (2006) 69–80.
[21] S. Mitra, A. Ghanbari-Siahkali, P. Kingshott, H.K. Rehmeier, H. Abildgaard, K. Almdal, Polym. Degrad. Stab. 91 (2006) 81–93.
[22] T. Sugama, Mater. Lett. 50 (2–3) (2001) 66–72.
[23] S. Mitra, A. Ghanbari-Siahkali, P. Kingshott, K. Almda, H.K. Rehmeier, A.G. Christensen, Polym. Degrad. Stab. 83 (2004) 195–206.
[24] M. Achenbach, Comp. Mater. Sci. 19 (2000) 213–222.
[25] M. Achenbach, Sealing Technology (2007) 10–13 (July).
[26] M. Achenbach, Sealing Technology (2007) 7–10 (August).
[27] M.S. Kim, J.H. Kim, J.K. Kim, S.J. Kim, Macromol. Res. 15 (4) (2007) 315–323.
[28] K.T. Gillen, RL. Clough, Irradiation Effects on Polymers, Elsevier Applied Science, London, 1991 (Chapter 4).
[29] J. Wise, K.T. Gillen, R.L. Clough, Polym. Degrad. Stab. 49 (1995) 403.
[30] K.T. Gillen, M. Celina, R.L. Clough, J. Wise, Trends Polym. Sci. 5 (1997) 250.
[31] K.T. Gillen, M.R. Keenan, J. Wise, Die Angewandte Makromolekulare Chemie 261–262 (1998) 83–92.
[32] K.T. Gillen, M. Celina, M.R. Keenan, Rubber Chem. Technol. 73 (2000) 265.
[33] K.T. Gillen, M. Celina, Polym. Degrad. Stab. 71 (2001) 15.
[34] K.T. Gillen, M. Celina, R. Bernstein, Polym. Degrad. Stab. 82 (2003) 25.
[35] K.T. Gillen, R. Bernstein, D.K. Derzon, Polym. Degrad. Stab. 87 (2005) 57.
[36] K.T. Gillen, R. Bernstein, M.H. Wilson, Polym. Degrad. Stab. 87 (2005) 257.
[37] K.T. Gillen, R. Bernstein, M. Celina, Polym. Degrad. Stab. 87 (2005) 335.
[38] M. Celina, K.T. Gillen, R.A. Assink, Polym. Degrad. Stab. 90 (2005) 395.
[39] K.T. Gillen, R. Bernstein, R.L. Clough, M. Celina, Polym. Degrad. Stab. 91 (2006) 2146.
[40] K.T. Gillen, M. Celina, R. Bernstein, M. Shedd, Polym. Degrad. Stab. 91 (2006) 3197.
[41] M. Schulze, T. Knori, A. Schneider, E. Gulzow, J. Power Sources 127 (1–2) (2004) 222–229.
[42] J. Tan, Y.J. Chao, W.K. Lee, C.S. Smith, J.W. Van Zee, C.T. Williams, Proceedings of the 4th international conference on fuel cell science, Engineering and Technology, June 19–21, Irvine, CA, 2006.
[43] J. Tan, Y.J. Chao, J.W. Van Zee, W.K. Lee, Mater. Sci. Eng. A 445–446 (2007) 669–675.
[44] J. Tan, Y.J. Chao, X. Li, J.W. Van Zee, J. Power Sources 172 (2) (2007) 782–789.
[45] J. Tan, Y.J. Chao, M. Yang, C.T. Williams, J.W. Van Zee, J. Mater. Eng. Performance 17 (2008) 785–792.
[46] J. Tan, Y.J. Chao, J.W. Van Zee, W.K. Lee, Mater. Sci. Eng. A (2008) 464–470.
[47] J. Tan, Y.J. Chao, H. Wang, J. Gong, J.W. Van Zee, Polym. Degrad. Stab. 94 (2009) 2072–2078.
[48] J. Tan, Y.J. Chao, X. Li, J.W. Van Zee, W.K. Lee, J. Fuel Cell Sci. Technol. 6 (2009), 041017(1–9).
[49] J. Tan, Y.J. Chao, M. Yang, W.K. Lee, J.W. Van Zee, Chemical and mechanical stability of a Silicone gasket material exposed to PEM fuel cell environment, Int. J. Hydrogen Energy (2009), doi:10.1016/j.ijhydene.2009.10.048.
[50] W.K. Lee, C.H. Ho, J.W. Van Zee, M. Murthy, J. Power Sources 84 (1999) 45–51.
[51] Dow Corning technical library, http://www.dowcorning.com.
[52] M.M. Green, H.A. Wittcoff, Organic Chemistry Principles and Industrial Practice, Wiley, Weinheim, Germany, 2003.
[53] D.K. Louie, Handbook of Sulphuric Acid Manufacturing, DKL Engineering Inc., Richmond Hill, Canada, 2005.
[54] AZom, Journal of Materials Online, http://www.azom.com.
[55] Lanxess Company, http://www.lanxess.com.
[56] ThomasNet, http://www.thomasnet.com/.
[57] Dupon Company, http://www.dupont.com/.
[58] D. Lin-Vien, N.B. Colthup, W.G. Fateley, J.G. Grasselli, The Handbook of Infrared and Raman Characteristic Frequencies of Organic Molecules, Academic Press, Boston, 1991.
[59] E.W. Colvin, Silicone in Organic Synthesis, Butterworth and Co. (Publishers) Ltd., Butterworths, 1981.
[60] A. Streiwieser Jr., C.H. Heathcock, Introduction to Organic Chemistry, Macmillian Publishing Co, New York, 1976.
[61] S. Yamazaki, Y. Katoa, I. Taniguchi, Surf. Sci. 7 (1) (1967) 68–78.
[62] Infrared Spectroscopy, http://www.spectroscopynow.com/.
[63] B. Tang, X.Q. Li, J.W. Wang (Eds.), EPDM rubber and applications, Chemical Industry Press, 2005 (in Chinese).
[64] N.S. Tomer, F. Delor-Jestin, R.P. Singh, J. Lacoste, Polym. Degrad. Stab. 92 (2007) 457–463.